Since January 2020 Elsevier has created a COVID-19 resource centre with free information in English and Mandarin on the novel coronavirus COVID-19. The COVID-19 resource centre is hosted on Elsevier Connect, the company's public news and information website.

Microchemical Journal 181 (2022) 107769

Contents lists available at ScienceDirect

Microchemical Journal

journal homepage: www.elsevier.com/locate/microc

Core shell stationary phase for a novel separation of some COVID-19 used drugs by UPLC-MS/MS Method: Study of grapefruit consumption impact on their pharmacokinetics in rats

Sally Tarek Mahmoud *, Marwa A. Moffid, Rawda M. Sayed, Eman A. Mostafa

Pharmaceutical Chemistry Department, Faculty of Pharmacy, Cairo University, Kasr El-Aini St., Cairo 11562, Egypt

ARTICLE INFO

Keywords:
COVID-19 Drugs
Pharmacokinetic Study
Grapefruit Juice
LC/MS/MS
Food-drug interaction
Rat Plasma

ABSTRACT

A sensitive and selective UPLC-MS/MS method was developed for the synchronized determination of four drugs used in severe acute respiratory syndrome coronavirus 2 (SARS-CoV-2), namely, azithromycin, apixaban, dexamethasone, and favipiravir in rat plasma. using a Poroshell 120 EC-C18 column (50 mm × 4.6 mm, 2.7 m) with a high-resolution ESI tandem mass spectrometer detection with multiple reaction monitoring. We used an Agilent Poroshell column, which is characterized by a stationary phase based on non-porous core particles. With a remarkable improvement in the number of theoretical plates and low column backpressure. In addition, the developed method was employed in studying the potential food-drug interaction of grapefruit juice (GFJ) with the selected drugs which affects their pharmacokinetics in rats. The LC-MS/MS operated in positive and negative ionization mode using two internal standards: moxifloxacin and chlorthalidone, respectively. Liquid- liquid extraction of the cited drugs from rat plasma was accomplished using diethyl ether: dichloromethane (70:30, *v/v*). The analytes were separated using methanol: 0.1 % formic acid in water (95: 5, *v/v*) as a mobile phase in isocratic mode of elution pumped at a flow rate of 0.3 mL/min. A detailed validation of the bio-analytical method was performed in accordance with US-FDA and EMA guidelines.

Concerning the *in vivo* pharmacokinetic study, the statistical significance between the results of the test groups receiving GFJ along with the cited drugs and the control group was assessed demonstrating that GFJ increased the plasma concentration of azithromycin, apixaban, and dexamethasone. Accordingly, this food–drug interaction requires cautious ingestion of GFJ in patients using (SARS-CoV-2) medications as it can produce negative effects in the safety of the drug therapy. A potential drug–drug interaction is also suggested between those medications requiring a suitable dose adjustment.

1. Introduction

Severe acute respiratory syndrome coronavirus 2 (SARS-CoV-2) which cause coronavirus disease 2019 (COVID-19) has become a pandemic disease since March 2020 [1,2]. Although the disease is not severe in most patients, it may develop a serious illness which may need hospitalization mainly in the elderly and those with underlying diseases [3,4]. The treatment strategies for COVID-19 contain medications approved for other viral diseases like Ebola, HIV, and influenza such as favipiravir, remdesivir, and ritonavir [5,6]. COVID-19 is associated with diffuse lung damage which may necessitate oxygen supply or even mechanical ventilation, glucocorticoids such as dexamethasone may control the inflammation-mediated lung injury and reduce mortality among the patients receiving either invasive mechanical ventilation or oxygen alone [7–9]. In addition, some studies reported that 50 % of deaths were due to secondary bacterial infections in patients hospitalized for COVID-19. Consequently, antibiotics is a crucial defense against mortality in COVID-19 patients [10]. Macrolides such as azithromycin were the most used in mild to moderate cases, with 29.1 % of patients [11–14]. Moreover, thrombotic cardiovascular complications and pneumonia-induced respiratory failure are increasingly emerging as a major COVID-19 symptom. Anticoagulant therapy has been strongly suggested from multiple retrospective studies as it improves the prognosis of people with COVID-19 [15–19]. In COVID-19 outpatients with cardiometabolic diseases, prior use of direct oral anti-coagulants such as: rivaroxaban or apixaban compared to vitamin K antagonists' therapy

* Corresponding author.
E-mail address: sally.mokhles@pharma.cu.edu.eg (S. Tarek Mahmoud).

https://doi.org/10.1016/j.microc.2022.107769
Received 22 April 2022; Received in revised form 11 June 2022; Accepted 6 July 2022
Available online 15 July 2022

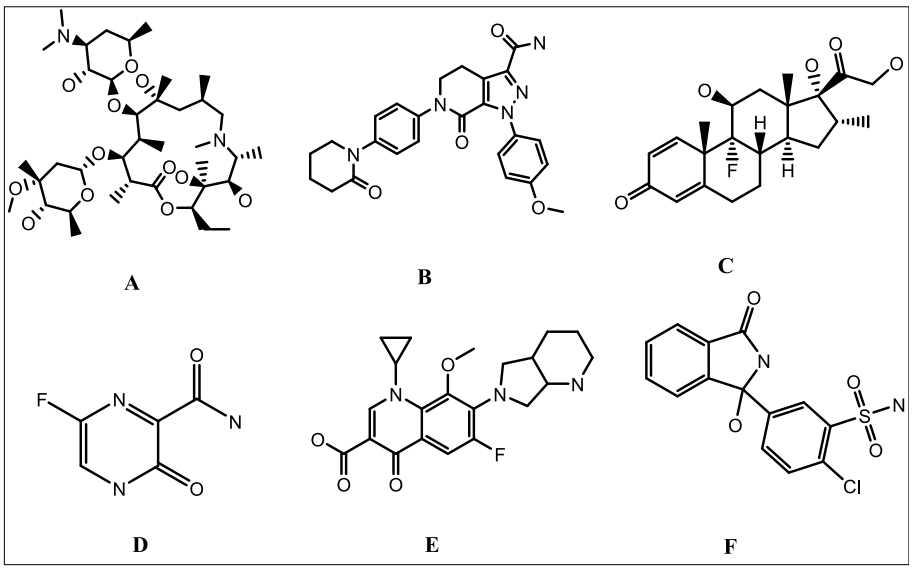

Fig. 1. Chemical structures of azithromycin (A), apixaban (B), dexamethasone (C), favipiravir (D), moxifloxacin (E), and chlorthalidone (F).

Table 1
MS/MS conditions for multiple reaction monitoring (MRM) of azithromycin, apixaban, dexamethasone, favipiravir, moxifloxacin and chlorthalidone in spiked rat plasma.

Analyte	Ionization mode	CE (V)	FV (V)	Precursor ion peak	Product ion peak	Dwell time (*sec*)
AZM	positive	30	45	749.47	591.38	0.029
APX	positive	25	35	460.17	443.09	0.029
DEX	negative	15	20	437.15	361.15	0.029
FAV	negative	25	25	155.97	112.92	0.029
MOX	positive	25	40	402.14	384.12	0.029
CHT	negative	15	35	337.04	189.60	0.029

CE: collision energy; FV: fragmentor voltage.

at the time of COVID-19 diagnosis demonstrated lower risk of arterial or venous thrombotic outcomes, without increasing the risk of bleeding [20].

Azithromycin (AZM), Fig. 1(A), is a nitrogen-containing 2nd generation macrolide antibacterial agent (azalide) with a wide-ranging spectrum of activity that inhibits bacterial protein synthesis. It is given in the treatment of respiratory tract infections (including bronchitis, pneumonia, sinusitis, trench fever, and otitis media), in skin and soft-tissue infections, and in uncomplicated genital infections [21,22].

Apixaban (APX), Fig. 1(B), is an oral anticoagulant which is direct, reversible, and potent inhibitor of factor Xa by selective blockage of its active site, [23–25]. It is used for the prevention of both stroke and systemic embolism in patients with non-valvar atrial fibrillation. In addition, it is used to prevent and treat deep vein thrombosis and pulmonary thromboembolism [26,27].

Dexamethasone (DEX), Fig. 1(C), is a potent synthetic glucocorticoid which is used as an anti-inflammatory and immunosuppressive agent [28]. It is used to treat a wide range of diseases as ulcerative colitis, arthritis, allergies and respiratory disorders [29,30]. Recently, it was proven that DEX is the main drug to show a life-saving efficacy of seriously ill COVID-19 patients by significantly improving their survival rate [9].

Favipiravir (FAV), Fig. 1(D), is a new oral antiviral drug used for management of influenza pandemic in Japan. It is a pro-drug that is subjected to ribosylation and phosphorylation intracellularly to form the active metabolite [31]. It selectively inhibits the viral RNA-dependent RNA polymerase enzymes, which are important for the transcription and replication of viral genomes. FAV has been also investigated for the treatment of Ebola virus, Lassa virus, and recently SARS-CoV-2 [32–34] where it showed higher efficacy in increasing the recovery rate and decreasing the incidence of fever and cough in COVID-19 patients [32,35].

Grapefruit belongs to the family Rutaceae and contains bioactive substances, such as flavonoids which has the functions of antioxidants, free radical elimination, tumor prevention, and rich in vitamin C, so it can be consumed with large quantities by COVID-19 patients. Numerous studies have shown that furocoumarin in grapefruit interacts with drugs by interfering with tactile and intestinal enzymes cytochrome P450 (CYP450) particularly the CYP3A4 [36–40]. Drugs transport with P-glycoprotein (P-gp) is also affected by the grapefruit's flavonoids [41,42]. These food-drug interactions can produce negative effects on the safety and efficacy of the drug therapy, as well as on the nutritional status of the patient [43].

Therefore, the aim of the presented study is to develop a validated UPLC-MS/MS method using a Poroshell 120 EC-C18 column whose stationary phase is based on recently developed non-porous core particles, for the separation of four drugs used in the management of COVID-19 in rat plasma and the application of the developed method to study the effect of the use of grapefruit juice (GFJ) on the pharmacokinetics (PK) of the four cited drugs.

Literature surveys revealed that different quantitative methods have been developed for analysis of individual components of the cited mixture. AZM was estimated in biological samples utilizing LC-UV [44,45], LC-MS [46,47], electrochemical [48,49] and spectrophotometric [50] methods. APX was determined in biological samples using LC-MS [26,51–56] and LC-DAD [57] methods. DEX was quantified in biological samples utilizing LC-MS [58–64], electrochemical [65] and spectrophotometric [66] methods, while FAV was quantified in biological samples utilizing LC-UV [67–70], LC-fluorometric [71], LC-MS [72–74], fluorometric [75], TLC [76], and electrochemical [77,78] methods. In addition, AZM and FAV were simultaneously determined in human serum utilizing LC-MS method [79].

To the best of our knowledge, there is no LC-MS/MS method for the

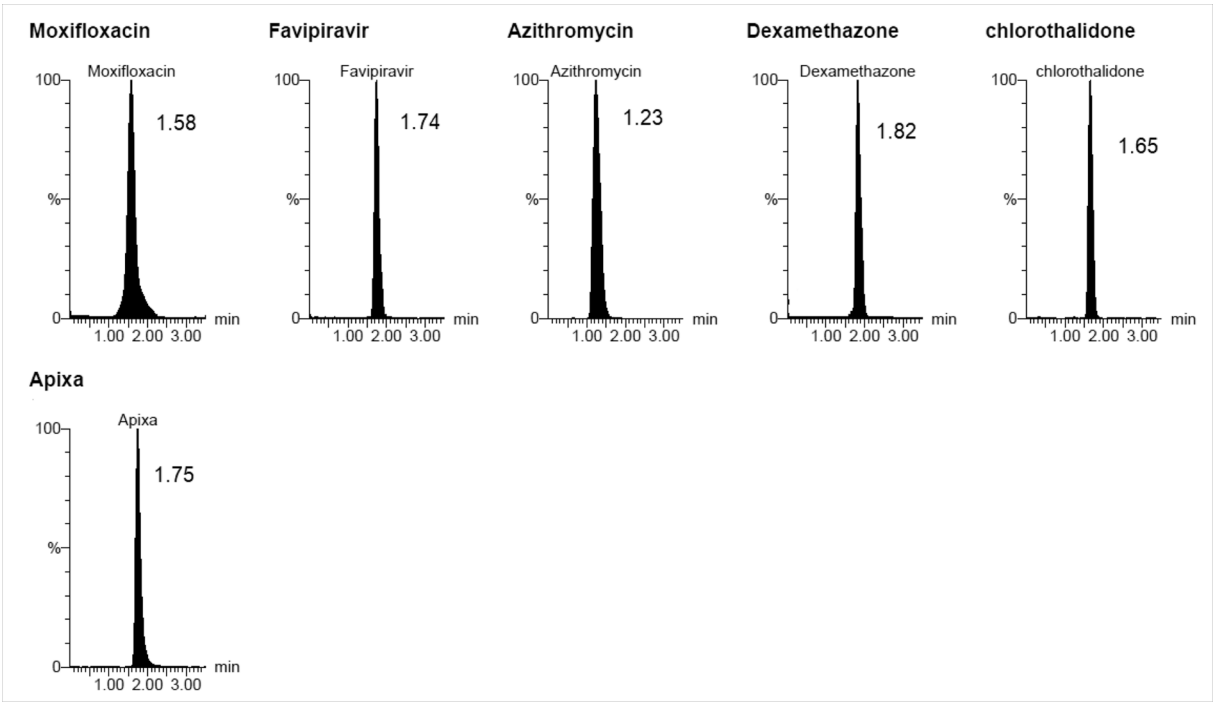

Fig. 2. MRM chromatograms of a 10 μL injection of lower limit of quantitation of azithromycin, apixaban, dexamethasone, favipiravir, moxifloxacin, and chlorthalidone.

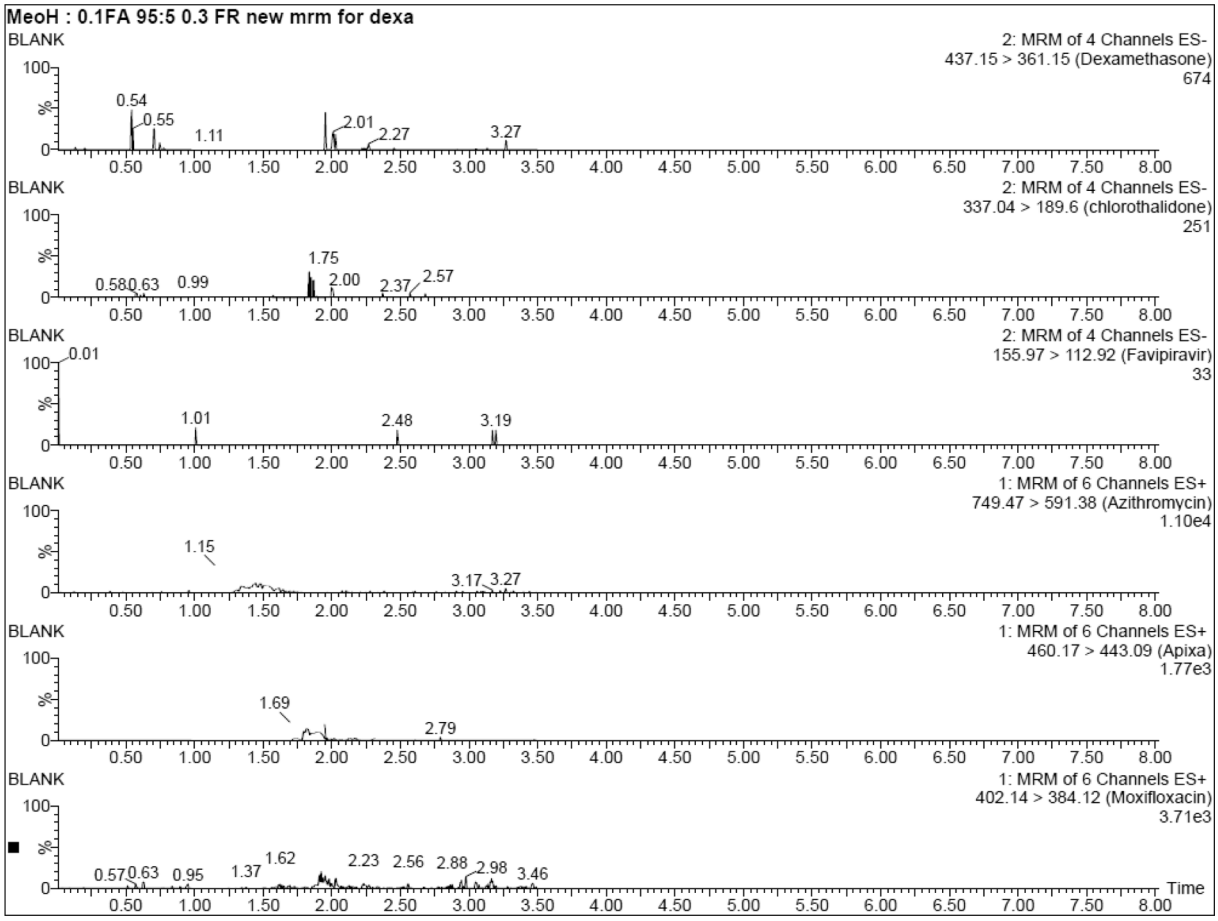

Fig. 3. MRM chromatogram of extracted drug-free rat plasma sample.

Table 2
Summary of back calculated standards of azithromycin, apixaban, dexamethasone, favipiravir in spiked rat plasma.

Conc. of drug in rat plasma	Accuracy (%)			
	AZM	APX	DEX	FAV
Level 1	105.00	104.09	82.91	103.45
Level 2	107.17	101.60	112.16	103.45
Level 3	109.10	105.50	108.97	100.00
Level 4	95.72	102.40	108.54	101.72
Level 5	89.78	95.98	96.41	101.72
Level 6	103.98	105.67	97.07	97.59
Level 7	101.27	96.86	100.84	101.72
Level 8	99.34	100.31	–	–
Mean regression coefficient	0.9995	0.9996	0.9994	0.9993
Mean intercept	0.0177	0.0600	0.1338	0.0045
Mean slope	0.0060	44.1910	1.4522	0.0029

simultaneous determination of the selected COVID-19 medications with the advantage of studying the potential food-drug interaction of GFJ affecting the PK of those drugs.

2. Materials and methods

2.1. Instruments

An UPLC Waters® 3100 (USA) consisting of: vacuum degasser, gradient binary pump, and auto-sampler was employed. Waters Acuity® TQ was used as a detector. Data was acquired and processed using MassLynx Workstation software (4.1). The separation and quantitation were conducted on an Agilent® Poroshell 120EC C_{18} column (50 mm × 4.6 mm, 2.7 μm), (USA). Nylon membrane filter (0.2 μm) (Sigma-Aldrich Co., Germany) was used for filtration of the mobile phase. A vortex mixer (Stuart, UK), a centrifuge (OHAUS, Frontier 5706, Germany), an ultrasonic bath (Power Sonic 405, Human Lab Inc., Korea), and a concentrator (Eppendorf 5301, USA) were employed throughout the work.

2.2. Chemicals, reference samples and solvents

AZM, APX, DEX, FAV, moxifloxacin (MOX), Fig. 1(G), and chlorthalidone (CHT), Fig. 1(H), were obtained from the National Organization of Drug Control and Research (NODCAR), Egypt (certified to contain 99.80 %, 99.75 %, 99.93 %, 99.85 %, 99.95 % and 99.92 %, respectively). Methanol, diethyl ether (DEE), dichloromethane (DCM), formic acid, and water were of HPLC grade and were purchased from Sigma-Aldrich Co., Germany. Carboxymethyl cellulose and tween 80 were purchased from El-Nasr Pharmaceutical Chemicals Co., Abu Zaabal, Al-Kalubia, Egypt. Drug-free rat plasma was prepared from blood samples collected in heparinized tubes.

2.3. LC-MS/MS conditions

Chromatographic separation was performed using an Agilent® Poroshell 120EC C_{18} column (50 mm × 4.6 mm, 2.7 μm) with a mobile phase consisting of methanol: 0.1 % formic acid in water (95: 5, *v/v*) at a flow rate of 0.3 mL/min. The injection volume was 10 μL and the injector needle wash solvent was water: methanol (50:50, *v/v*). The positive ion mode for the detection of AZM, APX, and MOX and the negative ion mode for the detection of DEX, FAV, and CHT, were selected using the Waters Acuity® TQ detector. Multiple Reaction Monitoring (MRM) transitions were measured. Tandem mass parameters are presented in Table 1. Peak area ratio was calculated for each drug using MOX as the IS for the positively ionized drugs and CHT for the negatively ionized drugs. MRM chromatograms of a 10 μL injection of LLOQ samples of the cited drugs are shown in Fig. 2.

Table 3
A summary of the validation results of the proposed LC-MS/MS method for azithromycin and apixaban.

Parameter	Results					
	AZM			APX		
Linearity: coefficient of determination (r^2)	0.9995			0.9996		
Calibration curve range	(0.001–1.5) μg/mL			(0.001–2.5) μg/mL		
Lower limit of quantitation	*1 ng/mL*			*1 ng/mL*		
QC level	*LQC (0.003 μg/mL)*	*MQC (0.6 μg/mL)*	*HQC (1.2 μg/mL)*	*LQC (0.003 μg/mL)*	*MQC (0.9 μg/mL)*	*HQC (2 μg/mL)*
Inter-day accuracy (%)	*96.48*	*96.82*	*101.84*	*100.90*	*97.64*	*94.39*
Inter-day precision (CV %)	*12.54*	*13.93*	*10.89*	*9.47*	*4.10*	*3.26*
Intra-day accuracy (%)	*98.15*	*102.01*	*95.79*	*98.29*	*95.73*	*94.77*
Intra-day precision (CV %)	*10.47*	*9.45*	*9.02*	*4.17*	*2.27*	*2.44*
Recovery of analyte (mean % recovery)	*89.15*	*89.58*	*90.65*	*93.03*	*90.87*	*98.79*
Short–term stability (6 hrs) (% accuracy)	*92.99*	–	*105.61*	*102.98*	–	*104.40*
Long–term stability (21 day) (% accuracy)	*104.07*	–	*95.63*	*94.59*	–	*95.50*
Auto-sampler stability (6 hrs) (% accuracy)	*105.74*	–	*110.23*	*108.87*	–	*90.37*
Freeze and thaw stability (% accuracy)	*102.96*	–	*104.36*	*100.00*	–	*92.41*
Matrix factor (mean)	*0.87*	–	*1.06*	*0.99*	–	*0.95*
IS normalized matrix factor (mean)	*1.01*	–	*1.13*	*1.15*	–	*1.05*
Stock solution stability (% stability ± CV%)	***6 hrs*** ***21 days***	*96.64 ± 2.63* *102.00 ± 1.09*		*99.08 ± 1.92* *98.59 ± 2.37*		
IS stock solution stability (% stability ± CV%)	***6 hrs*** ***21 days***	*101.78 ± 11.90* *96.52 ± 4.78*				
Dilution integrity (%accuracy ± CV%)	***2-fold*** ***10-fold***	*92.94 ± 3.72* *100.64 ± 6.82*		*98.80 ± 4.98* *95.12 ± 4.28*		

CV: Coefficient of Variation.

2.4. Standard solutions preparation

Standard stock solutions of (1 mg/mL) of AZM, APX, and DEX and (2 mg/mL) of FAV, were separately prepared in methanol. Working solutions were prepared by appropriate dilutions of the standard stock solution of each drug. MOX and CHT stock solutions (100 μg/mL) were also prepared using methanol. The working solutions of MOX and CHT, (5 μg/mL) and (1 μg/mL), respectively, were prepared. All working solutions were also prepared in methanol and stored under refrigeration (2–8 °C) along with the stock solutions.

Table 4
A summary of the validation results of the proposed LC-MS/MS method for dexamethasone and Favipiravir.

Parameter	*Results*					
	DEX			*FAV*		
Linearity: coefficient of determination (r^2)	0.9994			0.9993		
Calibration curve range	(0.05–10) μg/mL			(0.5–70) μg/mL		
Lower limit of quantitation	*50 ng/mL*			*500 ng/mL*		
QC level	*LQC (0.15 μg/mL)*	*MQC (4 μg/mL)*	*HQC (8 μg/mL)*	*LQC (1.5 μg/mL)*	*MQC (25 μg/mL)*	*HQC (55 μg/mL)*
Inter-day accuracy (%)	*104.49*	*104.56*	*103.63*	*101.92*	*98.53*	*103.96*
Inter-day precision (CV %)	*3.44*	*7.70*	*4.84*	*9.39*	*2.81*	*3.58*
Intra-day accuracy (%)	*101.76*	*100.88*	*98.11*	*109.58*	*97.29*	*106.79*
Intra-day precision (CV %)	*1.45*	*1.80*	*2.47*	*6.74*	*1.20*	*1.88*
Recovery of analyte (mean % recovery)	*90.80*	*89.96*	*93.64*	*91.41*	*94.53*	*94.05*
Short–term stability (6 hrs) (% accuracy)	*100.36*	–	*95.33*	*113.13*	–	*95.74*
Long–term stability (21 day) (% accuracy)	*95.07*	–	*110.99*	*95.02*	–	*106.06*
Auto-sampler stability (6 hrs) (% accuracy)	*94.16*	–	*103.34*	*109.58*	–	*102.15*
Freeze and thaw stability (% accuracy)	*109.72*	–	*99.93*	*105.75*	–	*102.03*
Matrix factor (mean)	*0.88*	–	*0.94*	*0.99*	–	*0.95*
IS normalized matrix factor (mean)	*1.01*	–	*1.08*	*1.05*	–	*0.99*
Stock solution stability (% stability ± CV %)	***6 hrs***	*92.17 ± 3.21*	*93.75 ± 1.54*			
	21 days	*100.43 ± 5.07*	*100.00 ± 1.44*			
IS stock solution stability(% stability ± CV %)	***6 hrs***	*96.18 ± 7.63*				
	21 days	*94.53 ± 4.25*				
Dilution integrity (% accuracy ± CV%)	***2-fold***	*93.69 ± 5.60*	*106.15 ± 2.63*			
	10-fold	*104.23 ± 3.12*	*97.22 ± 2.70*			

CV: Coefficient of Variation.

2.5. Calibrators and quality control samples preparation

Eight calibration levels were chosen covering the concentration ranges of (0.001–1.5 μg/mL) for AZM, and (0.001–2.5 μg/mL) for APX, while seven calibration levels were chosen covering the concentration ranges of (0.05–10 μg/mL) for DEX, and (0.5–70 μg/mL) for FAV. The samples were prepared by addition of 20 μL of known working solution, and 20 μL of MOX in case of AZM and APX samples or 20 μL of CHT in case of DEX and FAV samples, to 180 μL of drug-free rat plasma. Quality control (QC) samples were prepared at three levels – low (LQC): (0.003, 0.15, and 1.5 μg/mL) for AZM, APX, DEX, and FAV, respectively, medium (MQC): (0.6, 0.9, 4, and 25 μg/mL) for AZM, APX, DEX, and FAV, respectively, and high (HQC): (1.2, 2, 8, and 55 μg/mL) for AZM, APX, DEX, and FAV, respectively. All samples were vortexed for 1 min before extraction ensuring the complete mixing.

2.6. Sample preparation and extraction

Blank plasma was thawed at room temperature (RT) and then was vortexed for 30 s. A volume of 180 μL of drug-free rat plasma was spiked with 20 μL of the drug, and 20 μL of either MOX or CHT and vortexed for 1 min. Then, 2 mL of DEE: DCM (70: 30, *v/v*) were added, vortexed for 1 min and centrifuged at 3000 rpm, at 25 °C for 10 min. Afterwards, 1.5 mL of the organic layer was withdrawn and evaporated to dryness using vacuum concentrator at 45 °C, then the residue was reconstituted by 200 μL methanol and vortexed for 30 s. Ten μL of each of the resulting solutions were transferred to a glass vials for LC-tandem mass analysis.

2.7. Bio-analytical method validation

A detailed bio-analytical method validation was performed as per US-FDA [80] and EMA guidelines [81].

2.7.1. Selectivity

Six random drug-free plasma samples were collected from six different rats, processed using the aforementioned extraction procedure, and chromatographed. Blank plasma MRM chromatograms were compared with the MRM chromatograms of the LLOQ sample of each drug to determine the influence of endogenous plasma components which may cause interference at the retention time or the *m/z* channels of the analytes and the two IS, (Fig. 3).

2.7.2. Linearity

Calibration levels were prepared by spiking 180 μL of drug-free rat plasma with 20 μL of respective working solution of the cited drugs, and 20 μL of either MOX or CHT working solutions.

Three calibration curves were constructed each consisting of a blank sample, a zero sample and 8 non-zero samples of AZM and APX, and 7 non-zero samples of DEX and FAV covering the expected concentration range for each drug.

2.7.3. Recovery

Recovery (extraction efficiency) from rat plasma matrix was evaluated by comparing the mean peak areas of three extracted QC samples of the three QC levels to the mean peak areas of the corresponding un-extracted standards prepared in methanol. The recoveries of the 2 IS were also calculated in the same manner.

2.7.4. Matrix effect

The effect of the matrix components on ionization was investigated at LQC and HQC by calculation of both the matrix factor (MF) of each drug and IS and the IS normalized MF. The MF was calculated using six different post spiked plasma samples and the mean peak areas were compared to the mean peak areas of the corresponding neat solutions of equivalent concentrations prepared in methanol. The normalized MF was calculated by dividing the MF of each drug by the MF of the IS.

2.7.5. Accuracy and precision

Within-run and between-run accuracy and precision were assessed by six-replicate analyses of each analyte at the following levels: LLOQ QC, LQC, MQC, and HQC samples in spiked rat plasma in the same day and on three consecutive days, respectively. Percent accuracy (accuracy %) and percent coefficient of variation (CV %) were calculated.

2.7.6. Dilution integrity

Dilution integrity was evaluated by spiking the rat plasma matrix

Table 5
Pharmacokinetic parameters of azithromycin (30 mg/kg) and apixaban (5 mg/kg) after oral administration without and with grapefruit juice (n = 6).

Parameter	Control group (n = 6) (mean ± SD)		Test group (n = 6) (mean ± SD)		Unpaired student *t*-test	Calculated *p*-value	
	AZM	APX	AZM	APX		AZM	APX
C_{max} (μg/ml)	0.015 ± 6.05	0.005 ± 0.000	0.044 ± 8.77	0.16 ± 0.02	2.57	**0.018**	**0.005**
T_{max} (hr)	0.50 ± 0.00	0.50 ± 0.00	0.50 ± 0.00	0.50 ± 0.00	2.57	0.698	0.424
$t_{½}$ (hr)	10.65 ± 6.40	1.98 ± 0.25	8.90 ± 1.76	4.14 ± 1.46	2.57	0.692	0.127
$AUC_{(0-24)}$ (μg.hr/ml)	64.95 ± 32.66	0.01 ± 0.00	651.78 ± 217.63	0.05 ± 0.03	2.57	**0.044**	0.158
Cl (mg/kg)/(μg/ml)/h	0.42 ± 0.44	462.77 ± 43.18	0.03 ± 0.03	114.18 ± 52.87	2.57	0.258	**0.003**
V_d (mg/kg)/(μg/ml)	4.40 ± 0.48	1323.49 ± 241.23	0.35 ± 0.32	684.30 ± 424.23	2.57	**0.001**	0.108

*$p < 0.05$ indicates significant differences between the test and the control.
**C_{max}, maximum plasma concentration; T_{max}, time to Cmax; $t_{1/2}$, half-life; $AUC_{0-24,}$ Area under the curve from zero to 24 h; Cl, total body clearance; Vd, volume of distribution.

Table 6
Pharmacokinetic parameters of dexamethasone (8 mg/kg) and favipiravir (300 mg/kg) after oral administration without and with grapefruit juice (n = 6).

Parameter	Control group (n = 6) (mean ± SD)		Test group (n = 6) (mean ± SD)		Unpaired student *t*-test	Calculated *p*-value	
	DEX	FAV	DEX	FAV		DEX	FAV
C_{max} (μg/ml)	0.78 ± 0.25	59.14 ± 19.58	7.92 ± 2.17	67.76 ± 21.19	2.57	**0.030**	0.641
T_{max} (hr)	0.50 ± 0.00	0.50 ± 0.00	1.67 ± 0.58	0.67 ± 0.29	2.57	0.074	0.411
$t_{½}$ (hr)	4.16 ± 0.50	3.24 ± 3.05	6.74 ± 2.79	13.91 ± 9.37	2.57	0.255	0.202
$AUC_{(0-24)}$ (μg.hr/ml)	2.59 ± 2.22	99.94 ± 50.47	53.42 ± 17.37	345.47 ± 285.56	2.57	**0.037**	0.280
Cl (mg/kg)/(μg/ml)/h	4.24 ± 2.63	3.34 ± 1.50	0.15 ± 0.06	1.06 ± 0.89	2.57	0.115	0.109
V_d (mg/kg)/(μg/ml)	25.67 ± 17.72	12.36 ± 7.17	1.65 ± 1.27	13.40 ± 9.02	2.57	0.144	0.886

*$p < 0.05$ indicates significant differences between the test and the control.
**C_{max}, maximum plasma concentration; T_{max}, time to Cmax; $t_{1/2}$, half-life; $AUC_{0-24,}$ Area under the curve from zero to 24 h; Cl, total body clearance; Vd, volume of distribution.

with each analyte at a concentration above the upper limit of quantification (ULOQ) followed by diluting the samples with blank plasma using 2-fold and 10-fold dilution. The accuracy and the precision of the method were checked.

2.7.7. Stability

The LQC and HQC samples (n = 3, each) were used to assess the stability of the analytes in rat plasma. The obtained concentration, after application of the selected storage conditions, were compared to the nominal ones. Four storage conditions were selected to describe each operation within the analysis procedures.

Short-term stability (benchtop at RT for 6 h), long-term stability (deep freezer at (–70 ± 5 °C) for 21 days), auto-sampler stability (after reconstitution at RT in the auto-sampler for 6 h), freeze and thaw stability (three cycles, at each cycle, samples were frozen for at least 12 h before their unassisted thawing).

The stock solution stability of the four drugs and the two IS was evaluated by keeping the solutions for 21 days under refrigeration (2–8 °C) and for 6 h at RT (25–30 °C). Then, the mean peak area from six replicates was compared to the mean peak area of freshly prepared samples.

2.7.8. Carry-over:

The carry-over test was performed by injecting a blank rat plasma after injecting the calibration standard at ULOQ. The responses of each drug and the two IS were checked to confirm that the accuracy and precision of the method is not influenced.

2.8. Application of the proposed method to an in vivo pharmacokinetic interaction study

The study was approved by the Ethical Committee for Animal Experimentation at the Faculty of Pharmacy, Cairo University, Cairo, Egypt (No. PC3146). The study was conducted on 54 male Sprague-Dawley rats (weighting 200 g to 250 g). The rats were housed under standard laboratory conditions. Temperature was kept at 20–25 °C with humidity (50–60 %) for a minimum of 1 week prior to the study with free access to food and water. All rats were fasted the night before the beginning of the study but access to water was maintained.

Those rats were then randomly divided into 9 groups: 4 test groups, 4 control groups, and 1 group for the co-administration of the four drugs), each group is composed of 6 animals. The test groups were orally dosed with GFJ (5 mL/kg) once daily for 7 consecutive days and in the 8th day oral doses of each drug were given separately for each group at a dose of (30 mg/kg) of AZM, (5 mg/kg) of APX, (8 mg/kg) of DEX, and (300 mg/kg) of FAV to study the effect of GFJ on the PK of the 4 drugs. All drugs were formulated in 0.1 % carboxymethyl cellulose in water containing 4 % tween 80. On the other hand, the control groups were orally dosed with an equal volume of the vehicle for 7 consecutive days and in the 8th day oral doses of the investigated drugs were given separately for each group using the previously mentioned doses. The rats in the last 9th group were given the four drugs in mixture to study the effect of the drugs on the PK of each other. Then, the blood samples (0.25 mL) were collected from the *retro*-orbital plexus at different time intervals of (0, 0.25, 0.5, 1, 2, 4, 6, and 24 h) into Eppendorf tubes containing 50 μL heparin as anticoagulant. Plasma was prepared from these blood samples by centrifugation at 4000 rpm, at 25 °C for 10 min and kept at −70 °C till further analysis. Then, 200 μL of each plasma sample were separately spiked with 20 μL of MOX or CHT (IS) working solution, processed by the previously mentioned LLE procedure to be analyzed using the proposed UPLC–MS/MS method. The PK parameters were calculated using PKSolver add in in Microsoft Excel and the statistical significance of the PK parameters of test and control groups was evaluated applying unpaired Student *t*-test (two tailed), using Minitab® 18 software, and the *P*-values were calculated. A *P*-value < 0.05 was considered significant.

3. Results and discussion

Grapefruit juice (GFJ) consumption has numerous health benefits as

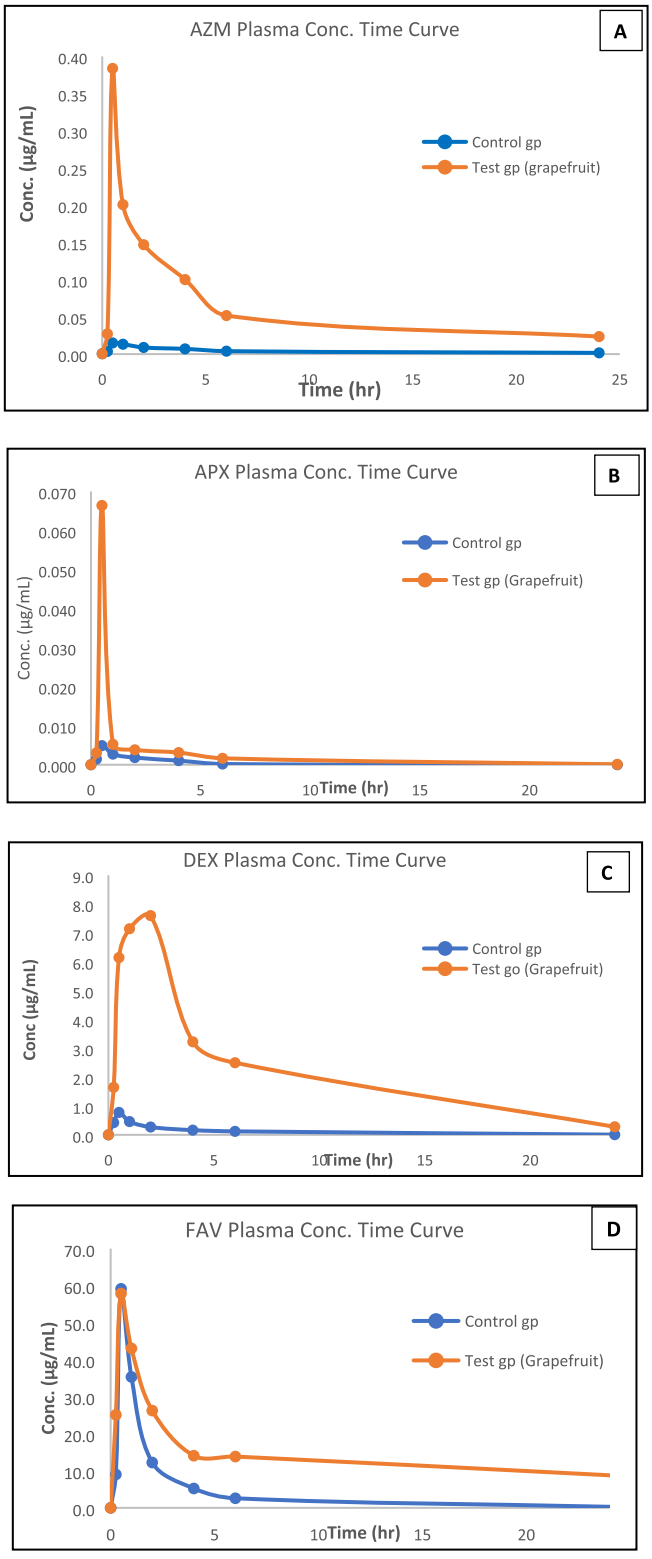

Fig. 4. The mean plasma concentration–time plot after oral administration of A) AZM, B) APX, C) DEX, D) FAV (dose 30, 5, 8, 300 mg/kg, respectively) alone or in combination with grapefruit juice in rats.

antioxidant, antiseptic, cardio-tonic, detoxicant, hypocholesterolemic, sedative [41] and a good source of vitamin C which has an important role in reducing the risk of severe respiratory distress in COVID-19 patients, reducing COVID-19 symptoms and its duration [82]. However, its intake is also associated with interactions with some drugs. Furanocoumarins of GFJ have inhibitory effect on the intestinal CYP450 mainly CYP3A4 enzyme, which mediates the intestinal first pass metabolism of many drugs. The P-gp, membrane transporter found in the brush border of the intestinal wall and the uptake transporters (e.g., organic anion-transporting polypeptides [OATPs]) are also affected by the flavonoids of GFJ. Based on these interactions, GFJ may alter the PK of many orally administered drugs, specifically the maximum plasma concentration (C_{max}) and the area under the drug concentration–time curve (AUC), by increasing their bioavailability [41,42].

Consequently, US-FDA advises against taking some medications with GFJ [83]. In spite of the US-FDA advice regarding the cautious ingestion of GFJ, many COVID-19 patients consume large quantities of GPJ as vitamin C rich source to improve their symptoms faster and decrease the risk of severe respiratory distress [82], and that may lead to interactions with the COVID-19 co-administered drugs. As a result of those findings, the objective of the presented study was to develop a fast, accurate and selective method to be used in the determination of the concentration of the selected drugs in rat plasma using UPLC-MS/MS. The developed method allows the determination of the four co-administered drugs used in the treatment of COVID-19 pandemic and study the effect of the concomitant consumption of GFJ which may affect the PK of the studied drugs. The selection of the linearity range of each drug was based on the C_{max} value of each drug in rat plasma [84–87].

3.1. Method development

3.1.1. Mass spectrometry

The goal of the optimization of MS/MS parameters was to increase the sensitivity of the method by maximizing the response for all the four drugs as well as the 2 IS. Tuning solutions of each drug and the 2 IS were separately injected. Both positive and negative electrospray ionization (ESI) were tried using several collision energies and fragmentor voltages to obtain the best sensitivity. MRM was used and the positive ionization mode was chosen for AZM and APX using MOX as IS. While the negative ionization mode was chosen for DEX and FAV using CHT as IS. Then, the following transitions were monitored: *m/z* 749.47 → 591.38 for AZM, *m/z* 460.17 → 443.09 for APX, *m/z* 437.15 → 361.15 for DEX, *m/z* 155.79 → 112.92 for FAV, *m/z* 402.14 → 384.12 for MOX and *m/z* 337.04 → 189.60 for CHT.

3.1.2. Optimization of sample extraction procedure

A simple precipitation technique was investigated using methanol and methanol: acetonitrile (50:50, *v/v*). Poor recoveries were obtained for the four cited drugs specially DEX and FAV. In addition, broad peaks were obtained. Thereafter, liquid–liquid extraction method was adopted using various organic solvents DEE, ethyl acetate (EA) and DEE: DCM (70:30, *v/v*). An improved extraction efficiencies for all the 4 drugs and the 2 IS were obtained using a mixture of DEE: DCM (70:30, *v/v*) giving the highest sensitivity of all tried extraction methods with optimum peaks shape.

Finding a suitable IS is a critical step in optimizing a bio-analytical method using LC-MS/MS, especially when there is ion mode switching between positive and negative ionization mode within the same chromatographic run.

Two challenges were encountered, the first was the choice of IS for the drugs using the positive mode and another IS for the drugs using the negative mode. The second challenge was to find that IS with a comparable recovery to the selected drugs using the same extraction method. Based on several trials, MOX and CHT were chosen for positive and negative ionization mode, respectively.

3.1.3. Chromatographic method development

Chromatographic separation was achieved using an Agilent® Poroshell 120EC C_{18} column (50 mm × 4.6 mm, 2.7 µm). The high efficiency of the non-porous core column for small molecules is owing to the combination of a reduced longitudinal diffusion parameter and Eddy

Table 7
Pharmacokinetic parameters of azithromycin (30 mg/kg) and apixaban (5 mg/kg) after oral administration alone and with co-administered drugs (n = 6).

Parameter	Control group (n = 6) (mean ± SD)		Test group (mixture of co-administrated drugs) (n = 6) (mean ± SD)		Unpaired student *t*-test	Calculated *p*-value	
	AZM	APX	AZM	APX		AZM	APX
C_{max} (μg/ml)	0.015 ± 6.05	0.005 ± 0.000	0.238 ± 17.51	0.14 ± 0.00	2.57	**0.002**	**0.001**
T_{max} (hr)	0.50 ± 0.00	0.50 ± 0.00	2.00 ± 0.00	4.00 ± 0.00	2.57	**0.000**	**0.002**
$t_{½}$ (hr)	10.65 ± 6.40	1.98 ± 0.25	7.19 ± 0.04	6.36 ± 0.21	2.57	0.448	**0.005**
$AUC_{(0-24)}$ (μg.hr/ml)	64.95 ± 32.66	0.01 ± 0.00	2353.55 ± 194.14	1.50 ± 0.04	2.57	**0.002**	**0.000**
Cl(mg/kg)/(μg/ml) /h	0.42 ± 0.44	462.77 ± 43.18	0.03 ± 0.02	3.08 ± 0.03	2.57	0.259	**0.019**
V_d(mg/kg)/ (μg/ml)	4.40 ± 0.48	1323.49 ± 241.23	0.14 ± 0.01	29.95 ± 0.51	2.57	**0.004**	**0.019**

*$p < 0.05$ indicates significant differences between the test and the control.
**C_{max}, maximum plasma concentration; T_{max}, time to Cmax; $t_{1/2}$, half-life; AUC_{0-24}, Area under the curve from zero to 24 h; Cl, total body clearance; Vd, volume of distribution.
***Mixture of co-administrated drugs (30 mg/kg AZM, 5 mg/kg APX, 8 mg/kg DEX and 300 mg/kg FAV).

Table 8
Pharmacokinetic parameters of dexamethasone (8 mg/kg) and favipiravir (300 mg/kg) after oral administration alone and with co-administered drugs (n = 6).

Parameter	Control group (n = 6) (mean ± SD)		Test group (mixture of co-administrated drugs) (n = 6) (mean ± SD)		Unpaired student *t*-test	Calculated *p*-value	
	DEX	FAV	DEX	FAV		DEX	FAV
C_{max} (μg/ml)	0.78 ± 0.25	59.14 ± 19.58	4.98 ± 0.25	65.71 ± 0.48	2.57	**0.000**	0.620
T_{max} (hr)	0.50 ± 0.00	0.50 ± 0.00	4.00 ± 0.00	2.00 ± 0.00	2.57	**0.049**	**0.000**
$t_{½}$ (hr)	4.16 ± 0.50	3.24 ± 3.05	6.43 ± 0.28	5.23 ± 0.08	2.57	**0.006**	0.377
$AUC_{(0-24)}$ (μg.hr/ml)	2.59 ± 2.22	99.94 ± 50.47	17.70 ± 0.01	156.82 ± 0.87	2.57	**0.007**	0.190
Cl (mg/kg)/(μg/ml)/h	4.24 ± 2.63	3.34 ± 1.50	0.38 ± 0.03	1.53 ± 0.38	2.57	0.126	0.180
V_d (mg/kg)/(μg/ml)	25.67 ± 17.72	12.36 ± 7.17	3.88 ± 0.02	14.58 ± 0.02	2.57	0.167	0.645

*$p < 0.05$ indicates significant differences between the test and the control.
**C_{max}, maximum plasma concentration; T_{max}, time to Cmax; $t_{1/2}$, half-life; AUC_{0-24}, Area under the curve from zero to 24 h; Cl, total body clearance; Vd, volume of distribution.
***Mixture of co-administrated drugs (30 mg/kg AZM, 5 mg/kg APX, 8 mg/kg DEX and 300 mg/kg FAV).

diffusion coefficient of the Van Deemter equation.

Different mobile phase compositions were tested in different ratios using an isocratic mode of elution using 0.1 % aqueous formic acid and ammonium formate buffer as aqueous phase, with acetonitrile and methanol as the organic modifier. The use of 0.1 % aqueous formic acid had the advantage of getting symmetrical, well-defined peaks and maximize detection response for all drugs more than the use of ammonium formate buffer. Also, the use of methanol showed better peaks shape and higher responses than the use of acetonitrile. Then, the ratio of methanol and 0.1 % aqueous formic acid was optimized to get the highest sensitivity and fast runtime.

As a result, the separation and quantitation were done using a mobile phase of methanol: 0.1 % formic acid (95: 5, *v/v*) pumped through an Agilent® Poroshell 120EC C_{18} column (50 mm × 4.6 mm, 2.7 μm) at a flow rate of 0.3 mL/min. The following retention times were obtained for AZM, APX, DEX, FAV, MOX, and CHT were around 1.23, 1.75, 1.82, 1.74, 1.58, and 1.65, min, respectively, in a total run time of 2 min, (Fig. 2).

3.2. Bio-analytical method validation

According to the acceptance criteria in US-FDA guidelines [80] and EMA guidelines [81], the allowed deviation from the nominal concentration was not more than ±15.0 % for both accuracy % and CV % of all of the LQC, MQC and HQC and within ±20.0 % for LLOQ.

3.2.1. Selectivity

The selectivity of the method was assessed by the absence of the interferences from other blank rat plasma components in the retention time and MRM channels of the 4 analytes and the 2 IS. MRM chromatograms of the spiked and blank rat plasma samples are shown in Figs. 2 and 3 confirming the high selectivity of the proposed UPLC method.

3.2.2. Linearity

Three calibration curves were constructed at 8 non-zero concentration levels for AZM and APX and 7 non-zero concentration levels for DEX and FAV. The calibration curves were linear over the selected range of each drug. The regression equation for each cited drug was computed and the mean regression coefficients were found to be 0.9995, 0.9996, 0.9994, and 0.9993 for AZM, APX, DEX, and FAV, respectively, Table 2. Linearity of the method was also confirmed by the back calculated concentrations of the calibration standards which provide satisfactory results, Table 2.

3.2.3. Lower limit of quantitation

The LLOQ was established at (1, 1, 50, and 500 ng/mL) for AZM, APX, DEX, and FAV, respectively.

3.2.4. Recovery

The recovery of the analytes should be consistent and reproducible [80], Using the selected LLE technique with DEE: DCM (70: 30, *v/v*), good and reproducible recovery results were obtained for the 4 drugs from rat plasma, Tables 3 and 4. Similarly, the mean recoveries of the 2 IS (MOX and CHT) were calculated and found to be 93.76 ± 2.16 % and 91.00 ± 2.19 %, respectively.

3.2.5. Matrix effect

No matrix effect was observed, indicating that there are no interfering components within the matrix that could affect the ionization of the 4 analytes or the 2 IS. Both MF and IS normalized MF were calculated for each drug at the LQC and HQC, Table 3 and 4.

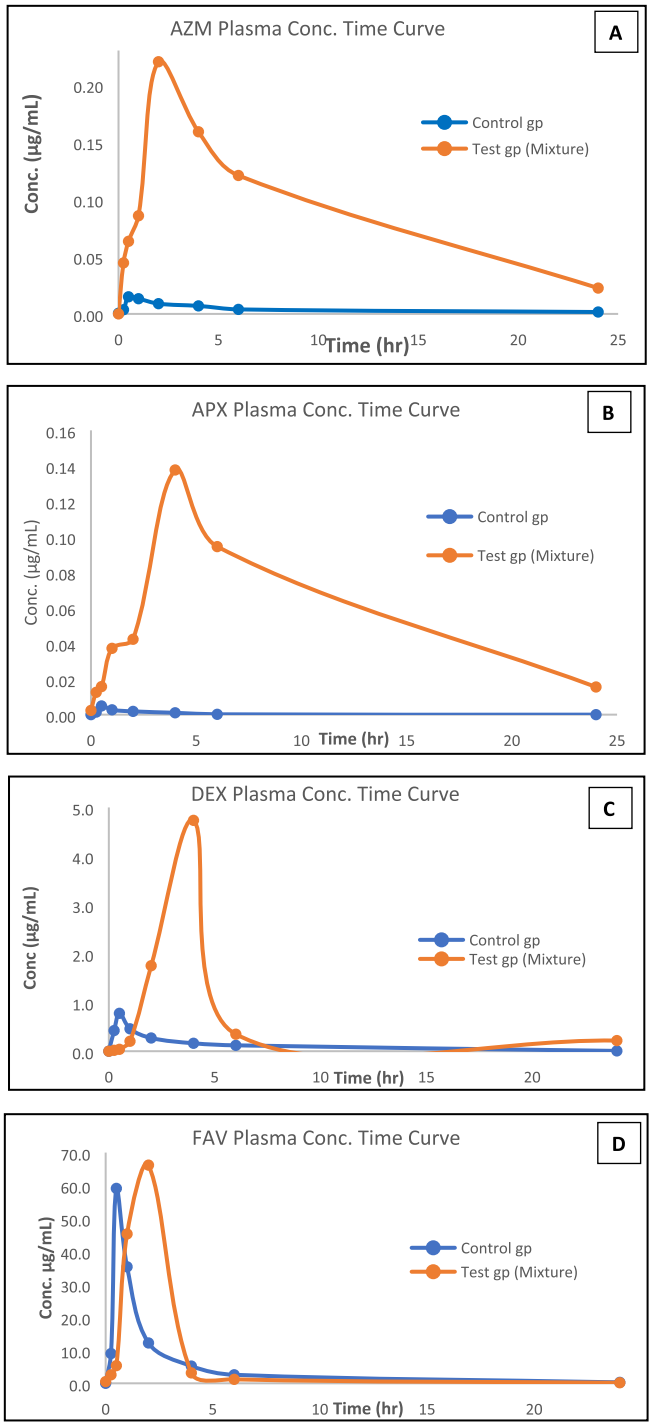

Fig. 5. The mean plasma concentration–time plot after oral administration of A) AZM, B) APX, C) DEX, D) FAV (dose 30, 5, 8, and 300 mg/kg, respectively) alone or in combination with each other's in rats.

3.2.6. *Accuracy and precision*

Both accuracy % and CV % were calculated for each drug using the 4 QC levels to represent the accuracy and the precision of the method, respectively. Within-run and between-run accuracy and precision results are presented in Tables 3 and 4.

3.2.7. *Dilution integrity*

The measured concentrations of each drug in rat plasma following the dilution integrity test either 2-fold or 10-fold dilutions were within satisfactory results, Tables 3 and 4.

3.2.8. *Stability*

All drugs were found to be stable in rat plasma matrix concerning the selected storage conditions: short-term, long-term, auto-sampler, and freeze and thaw stability. Accuracy % results of stability samples are presented in Tables 3 and 4. For, stock solution stability, CV % and stability % of the 4 drugs and the 2 IS were calculated and presented in Tables 3 and 4.

3.2.9. *Carry-over*

No significant peak ≥20 % of the LLOQ or 5 % of the IS was observed in blank plasma samples injected after the ULOQ samples.

3.3. *Application of the proposed method in in vivo pharmacokinetic interaction study*

The developed UPLC–MS/MS method was used to determine the plasma concentration in the study of the *in vivo* PK of AZM, APX, DEX, and FAV after their oral administration either in case of concomitant consumption of GFJ or in case of their co-administration in Sprague–Dawley rats. Plasma samples of DEX and FAV with high concentration (above the ULOQ) were subjected to dilution using blank plasma to make the concentration within the selected linearity range. It's worth mentioning that there was no interference arousing from the components from GFJ at the retention times of the selected drugs or the 2 IS.

The results of the effects of GFJ consumption on the PK parameters of AZM, APX, DEX, and FAV are presented in Tables 5 and 6. As shown in Table 5 and 6, the concomitant consumption of GFJ caused a significant increase in the mean C_{max} and the mean AUC $_{(0-24)}$ of AZM and DEX and the mean C_{max} of APX indicating an increase in their absorption through GIT while FAV was almost unaffected by GFJ consumption.

The results revealed a significant increase in the mean C_{max} and the mean AUC $_{(0\ -2\ 4)}$ for AZM (3 folds increase and 10 folds increase, respectively), while there was a significant decrease in the mean V_d for AZM (13 folds decrease). For APX, a significant increase of the mean C_{max} (32 folds increase) was observed, along with a significant decrease in Cl (4 folds decrease). For DEX, a 10 folds increase and 21 folds increase were observed in the mean C_{max} and the mean AUC $_{(0-24)}$, respectively. The significant increase in the mean C_{max} and the mean AUC with a nonsignificant change in T_{max} and $t_{1/2}$ indicate an inhibition of intestinal CYP3A4 rather than hepatic CYP3A4 enzymes.

These findings are consistent with the fact that GFJ inhibit the activity of intestinal CYP3A4 and P-gp in the brush border of the intestinal walls, increasing the systemic exposure by increasing the extent of absorption of AZM, APX, and DEX which are metabolized by CYP3A4 enzyme and are substrates of P-gp [88–98].

While FAV is neither a substrate of P-gp nor a substrate of CYP3A4, it is metabolized by aldehyde oxidase enzyme and CYP2C8 enzyme [99]. As a result, its PK parameters were not affected by the concomitant consumption of GFJ.

The overlain plasma concentration -time profile of each drug alone and with GFJ juice was constructed by plotting the plasma concentration in µg/mL vs time in hours proving the aforementioned findings, Fig. 4.

Based on the above findings, the concomitant use of GFJ with AZM, APX, and DEX for the treatment of COVID-19 or any other illness should be avoided or used with caution to avoid this potential food-drug interaction as it may increase their systemic plasma exposure resulting in an increased risk of causing adverse effects.

Furthermore, co-administration of the selected drugs caused significant changes in the PK parameters of AZM, APX, and DEX, Tables 7 and 8.

Table 7 shows a significant increase in the mean C_{max}, and the mean AUC $_{(0-24)}$ (16 folds increase and 36 folds increase, respectively), with a significant increase in the mean T_{max} (4 folds increase while a significant decrease was observed in the mean V_d (31 folds decrease) for AZM. For APX, a significant increase in the mean C_{max} (28 folds increase), the mean AUC $_{(0-24)}$ (150 folds increase), the mean T_{max} (8 folds increase)

and the mean $t_{1/2}$ (3 folds increase) while there was a significant decrease in the mean Cl (150 folds decrease) and the mean V_d (44 folds decrease). Table 8 shows a significant increase in the mean C_{max} and the mean AUC $_{(0-24)}$ (6 folds increase and 7 folds increase, respectively) with a significant increase in the mean T_{max} and $t_{1/2}$ (8 folds increase and 1.5 folds increase, respectively) for DEX.

From the obtained PK results, it is shown that the co-administration of the cited dugs resulted in a statistically significant changes in their PK parameters in rats suggesting potential drug-drug interactions requiring dose adjustment to avoid any possible side effects.

Fig. 5 shows the overlain plasma concentration -time profile of each drug alone and when the 4 drugs were co-administered.

The possible consequences of these changes in the PK of the cited drugs either upon co-administration or upon concomitant consumption of GFJ need to be furtherly investigated in humans to assess their clinical significance.

4. Conclusion

A fast, accurate, and selective UPLC–MS/MS method was developed for determination of four drugs commonly used in the treatment of COVID-19 namely, azithromycin, apixaban, dexamethasone, and favipiravir in rat plasma using LLE. The developed method was fully validated according to US-FDA and EMA guidelines. The method was successfully applied to study the effect of concomitant administration of grapefruit juice on the pharmacokinetics of the cited drugs in Sprague–Dawley rats. In addition, the method was applied to study the effect of co-administration of those 4 drugs on the pharmacokinetics of each other. The results of the study suggest that the concomitant administration of grapefruit juice with the selected drugs could significantly increase the systemic exposure of AZM, APX, and DEX by increasing the extent of their absorption suggesting a potential food-drug interaction. Also, co-administration of those drugs could significantly increase their systemic exposure suggesting a potential drug-drug interaction.

CRediT authorship contribution statement

Sally Tarek Mahmoud: Conducting a research, Data curation, Formal analysis, or Interpretation of data for the work. **Marwa A. Moffid:** Conceptualization, Design of the work and final approval of the version to be published. **Rawda M. Sayed:** Writing – original draft, The work and revising it critically for important intellectual content. **Eman A. Mostafa:** Investigation, Validation, Supervision.

Declaration of Competing Interest

The authors declare that they have no known competing financial interests or personal relationships that could have appeared to influence the work reported in this paper.

References:

[1] C. Huang, Y. Wang, X. Li, L. Ren, J. Zhao, Y. Hu, L. Zhang, G. Fan, J. Xu, X. Gu, Z. Cheng, T. Yu, J. Xia, Y. Wei, W. Wu, X. Xie, W. Yin, H. Li, M. Liu, Y. Xiao, H. Gao, L. Guo, J. Xie, G. Wang, R. Jiang, Z. Gao, Q. Jin, J. Wang, B. Cao, Clinical features of patients infected with 2019 novel coronavirus in Wuhan China, Lancet 395 (2020) 497–506, https://doi.org/10.1016/S0140-6736(20)30183-5.

[2] N. Zhu, D. Zhang, W. Wang, X. Li, B. Yang, J. Song, X. Zhao, B. Huang, W. Shi, R. Lu, P. Niu, F. Zhan, X. Ma, D. Wang, W. Xu, G. Wu, G.F. Gao, W. Tan, A novel coronavirus from patients with Pneumonia in China, N. Engl. J. Med. 382 (2020) (2019) 727–733, https://doi.org/10.1056/NEJMOA2001017.

[3] W. Yang, Q. Cao, L.e. Qin, X. Wang, Z. Cheng, A. Pan, J. Dai, Q. Sun, F. Zhao, J. Qu, F. Yan, novel coronavirus disease (COVID-19): a multi-center study in Wenzhou city, Zhejiang, China, J. Infect. 80 (4) (2020) 388–393.

[4] COVID-19 Information for Specific Groups of People | CDC, (2019). https://www.cdc.gov/coronavirus/2019-ncov/need-extra-precautions/index.html.

[5] R.C. Becker, Covid-19 treatment update: follow the scientific evidence, J. Thromb. Thrombolysis. 50 (2020) 43–53, https://doi.org/10.1007/S11239-020-02120-9.

[6] C. Scavone, S. Brusco, M. Bertini, L. Sportiello, C. Rafaniello, A. Zoccoli, L. Berrino, G. Racagni, F. Rossi, A. Capuano, Current pharmacological treatments for COVID-19: what's next? Br. J. Pharmacol. 177 (2020) 4813–4824, https://doi.org/10.1111/bph.15072.

[7] J.P. Zhao, Y. Hu, R.H. Du, Z.S. Chen, Y. Jin, M. Zhou, J. Zhang, J.M. Qu, B. Cao, Expert consensus on the use of corticosteroid in patients with 2019-nCoV pneumonia, Zhonghua Jie He He Hu Xi Za Zhi. 43 (2020) 183–184, https://doi.org/10.3760/CMA.J.ISSN.1001-0939.2020.03.008.

[8] J.A.C. Sterne, S. Murthy, J.V. Diaz, A.S. Slutsky, J. Villar, D.C. Angus, D. Annane, L. C.P. Azevedo, O. Berwanger, A.B. Cavalcanti, P.-F. Dequin, B. Du, J. Emberson, D. Fisher, B. Giraudeau, A.C. Gordon, A. Granholm, C. Green, R. Haynes, N. Heming, J.P.T. Higgins, P. Horby, P. Jüni, M.J. Landray, A. Le Gouge, M. Leclerc, W.S. Lim, F.R. Machado, C. McArthur, F. Meziani, M.H. Møller, A. Perner, M.W. Petersen, J. Savovic, B. Tomazini, V.C. Veiga, S. Webb, J. C. Marshall, Association between administration of systemic corticosteroids and mortality among critically Ill patients with COVID-19 A meta-analysis, JAMA 324 (13) (2020) 1330.

[9] Dexamethasone in Hospitalized Patients with Covid-19, N. Engl. J. Med. 384 (2021) 693–704. https://doi.org/10.1056/NEJMOA2021436.

[10] F. Zhou, T. Yu, R. Du, G. Fan, Y. Liu, Z. Liu, J. Xiang, Y. Wang, B. Song, X. Gu, L. Guan, Y. Wei, H. Li, X. Wu, J. Xu, S. Tu, Y. Zhang, H. Chen, B. Cao, Clinical course and risk factors for mortality of adult inpatients with COVID-19 in Wuhan, China: a retrospective cohort study, Lancet 395 (2020) 1054–1062, https://doi.org/10.1016/S0140-6736(20)30566-3.

[11] M.G.S. Borba, F.F.A. Val, V.S. Sampaio, M.A.A. Alexandre, G.C. Melo, M. Brito, M. P.G. Mourão, J.D. Brito-Sousa, D. Baía-da-Silva, M.V.F. Guerra, L.A. Hajjar, R. C. Pinto, A.A.S. Balieiro, A.G.F. Pacheco, J.D.O. Santos, F.G. Naveca, M.S. Xavier, A.M. Siqueira, A. Schwarzbold, J. Croda, M.L. Nogueira, G.A.S. Romero, Q. Bassat, C.J. Fontes, B.C. Albuquerque, C.-T. Daniel-Ribeiro, W.M. Monteiro, M.V. G. Lacerda, Effect of high vs low doses of chloroquine diphosphate as adjunctive therapy for patients hospitalized with severe acute respiratory syndrome coronavirus 2 (SARS-CoV-2) infection A randomized clinical trial, J. Am. Med. Assoc. 3 (4) (2020) e208857, https://doi.org/10.1001/jamanetworkopen.2020.8857.

[12] J.P. Metlay, G.W. Waterer, A.C. Long, A. Anzueto, J. Brozek, K. Crothers, L. A. Cooley, N.C. Dean, M.J. Fine, S.A. Flanders, M.R. Griffin, M.L. Metersky, D. M. Musher, M.I. Restrepo, C.G. Whitney, Diagnosis and treatment of adults with community-acquired pneumonia, Am. J. Respir. Crit. Care Med. 200 (2019) e45–e67, https://doi.org/10.1164/rccm.201908-1581ST.

[13] H. Chen, J. Guo, C. Wang, F. Luo, X. Yu, W. Zhang, J. Li, D. Zhao, D. Xu, Q. Gong, J. Liao, H. Yang, W. Hou, Y. Zhang, Clinical characteristics and intrauterine vertical transmission potential of COVID-19 infection in nine pregnant women: a retrospective review of medical records, Lancet 395 (2020) 809–815, https://doi.org/10.1016/S0140-6736(20)30360-3.

[14] X.Y. Zhao, X.X. Xu, H. Sen Yin, Q.M. Hu, T. Xiong, Y.Y. Tang, A.Y. Yang, B.P. Yu, Z. P. Huang, Clinical characteristics of patients with, coronavirus disease in a non-Wuhan area of Hubei Province, China: a retrospective study, BMC Infect. Dis. 20 (2020) (2019) 1–8, https://doi.org/10.1186/S12879-020-05010-W/TABLES/4.

[15] M. Komiyama, K. Hasegawa, Anticoagulant therapy for patients with coronavirus disease 2019: urgent need for enhanced awareness, Eur. Cardiol. Rev. 15 (2020), https://doi.org/10.15420/ECR.2020.24.

[16] T. Umapathi, A. Ching, K.N. Venketasubramanian, C.C. Tchoyoson, L. Boon, C. Pang, T. Tsai, Y. Cheng, C.L. Poh, L. Lim, K. Ponnudurai, K. Leong, C. Puay, H. Tan, D. Yeng, H. Tai, S. Peng, B. Ang, Large artery ischaemic stroke in severe acute respiratory syndrome (SARS), Springer 251 (2004) 1227–1231, https://doi.org/10.1007/s00415-004-0519-8.

[17] F.A. Klok, M.J.H.A. Kruip, N.J.M. van der Meer, M.S. Arbous, D.A.M.P.J. Gommers, K.M. Kant, F.H.J. Kaptein, J. van Paassen, M.A.M. Stals, M. V. Huisman, H. Endeman, Incidence of thrombotic complications in critically ill ICU patients with COVID-19, Thromb. Res. 191 (2020) 145–147. https://doi.org/10.1016/J.THROMRES.2020.04.013.

[18] J. Poissy, J. Goutay, M. Caplan, E. Parmentier, T. Duburcq, F. Lassalle, E. Jeanpierre, A. Rauch, J. Labreuche, S. Susen, N. Cousin, A. Durand, A. El Kalioubie, R. Favory, P. Girardie, M. Houard, E. Jaillette, M. Jourdain, G. Ledoux, D. Mathieu, A.-S. Moreau, C. Niles, S. Nseir, T. Onimus, S. Préau, L. Robriquet, A. Rouzé, A. Simonnet, S. Six, A. Toussaint, A. Dupont, A. Bauters, C. Zawadzki, C. Paris, N. Trillot, B. Wibaut, A. Hochart, C. Marichez, V. Dalibard, S. Vanderziepe, L. Bourgeois, A. Gaul, A. Jospin, N. Stepina, B. Pradines, A. Tournoys, T. Brousseau, M. Rémy, A. Hutt, Pulmonary embolism in patients with COVID-19: awareness of an increased prevalence, Circulation 142 (2) (2020) 184–186.

[19] N. Tang, H. Bai, X. Chen, J. Gong, D. Li, Z. Sun, Anticoagulant treatment is associated with decreased mortality in severe coronavirus disease 2019 patients with coagulopathy, J. Thromb. Haemost. 18 (2020) 1094–1099, https://doi.org/10.1111/jth.14817.

[20] J.M. Rivera-Caravaca, S.L. Harrison, B.J.R. Buckley, E. Fazio-Eynullayeva, P. Underhill, F. Marín, G.Y.H. Lip, Efficacy and safety of direct-acting oral anticoagulants compared to vitamin K antagonists in COVID-19 outpatients with cardiometabolic diseases, Cardiovasc. Diabetol. 20 (2021) 1–11, https://doi.org/10.1186/S12933-021-01368-6.

[21] S.C. Sweetman, Martindale: The Complete Drug Reference, 40th ed., Pharmaceutical Press, 2020.

[22] M.J. Parnham, V.E. Haber, E.J. Giamarellos-Bourboulis, G. Perletti, G.M. Verleden, R. Vos, Azithromycin: mechanisms of action and their relevance for clinical applications, Pharmacol. Ther. 143 (2014) 225–245, https://doi.org/10.1016/J.PHARMTHERA.2014.03.003.

[23] X. Jiang, E.J. Crain, J.M. Luettgen, W.A. Schumacher, P.C. Wong, Apixaban, an oral direct factor Xa inhibitor, inhibits human clot-bound factor Xa activity in vitro,

Thromb. Haemost. 101 (2009) 780–782, https://doi.org/10.1160/TH08-07-0486/ID/JR0486-11.
[24] J.M. Luettgen, R.M. Knabb, K. He, D.J.P. Pinto, A.R. Rendina, Apixaban inhibition of factor Xa: Microscopic rate constants and inhibition mechanism in purified protein systems and in human plasma, J. Enzyme Inhib. Med. Chem. 26 (2011) 514–526, https://doi.org/10.3109/14756366.2010.535793.
[25] F. Scaglione, F. Scaglione, New oral anticoagulants: comparative pharmacology with Vitamin K antagonists, Clin. Phar. 52 (2013) 69–82, https://doi.org/10.1007/s40262-012-0030-9.
[26] H.C. Jeong, T.E. Kim, K.H. Shin, Quantification of apixaban in human plasma using ultra performance liquid chromatography coupled with tandem mass spectrometry, Transl. Clin. Pharmacol. 27 (2019) 33–41. https://doi.org/10.12793/tcp.2019.27.1.33.
[27] Eliquis (Apixaban) Prescribing Information. Princeton, NJ and New York, NY: Bristol-Myers Squibb and Pfizer, (2015).
[28] S. Timmermans, J. Souffriau, C. Libert, A general introduction to glucocorticoid biology, Front. Immunol. 10 (2019) 1–17, https://doi.org/10.3389/FIMMU.2019.01545/FULL.
[29] B. Mukherjee, S. Mahapatra, R. Gupta, B. Patra, A. Tiwari, P. Arora, A comparison between povidone-ethylcellulose and povidone-eudragit transdermal dexamethasone matrix patches based on in vitro skin permeation, Eur. J. Pharm. Biopharm. 59 (2005) 475–483, https://doi.org/10.1016/J.EJPB.2004.09.009.
[30] L.B. Randa Hilal-Dandan, B. Knollmann, Goodman and Gilman's The Pharmacological Basis of Therapeutics, 13th ed.,, McGraw-Hill Education, 2017.
[31] Y. Furuta, T. Komeno, T.N. the J. Academy, S. B, U, Favipiravir (T-705), a broad spectrum inhibitor of viral RNA polymerase, Proc. Jpn. Acad. Ser. B. Phys. Biol. Sci. 93 (2017) (2017) 449–463, https://doi.org/10.2183/pjab.93.027.
[32] Q. Cai, M. Yang, D. Liu, J. Chen, D. Shu, J. Xia, X. Liao, Y. Gu, Q. Cai, Y. Yang, C. Shen, X. Li, L. Peng, D. Huang, J. Zhang, S. Zhang, F. Wang, J. Liu, L. Chen, S. Chen, Z. Wang, Z. Zhang, R. Cao, W. Zhong, Y. Liu, L. Liu, Experimental treatment with Favipiravir for COVID-19: an open-label control study, Engineering. 6 (2020) 1192–1198, https://doi.org/10.1016/J.ENG.2020.03.007.
[33] E.A.C., H. Haghbayan, Favipiravir, an antiviral for COVID-19?, J. Antimicrob. Chemother. 75 (2020) 2013–2014. https://doi.org/10.1093/jac/dkaa171.
[34] U. Agrawal, R. Raju, Z.F. Udwadia, Favipiravir: a new and emerging antiviral option in COVID-19, Med. J. Armed Forces India. 76 (2020) 370–376, https://doi.org/10.1016/J.MJAFI.2020.08.004.
[35] C. Chen, Y. Zhang, J. Huang, P. Yin, Z. Cheng, J. Wu, S. Chen, Y. Zhang, B. Chen, M. Lu, Y. Luo, L. Ju, J. Zhang, X. Wang, Favipiravir versus arbidol for COVID-19: A randomized clinical trial, MedRxiv. (2020) 2020.03.17.20037432. https://doi.org/10.1101/2020.03.17.20037432.
[36] E. Madrigal-Bujaidar, L.M. Roaro, K. García-Aguirre, S. Garcia-Medina, I. Alvarez-Gonzalez, Grapefruit juice suppresses azoxymethane-induced colon aberrant crypt formation and induces antioxidant capacity in mice, Asian Pac. J. Cancer Prev. 14 (2013) 6851–6856, https://doi.org/10.7314/APJCP.2013.14.11.6851.
[37] A.A. Mahgoub, Grapefruit juice potentiates the anti-inflammatory effects of diclofenac on the carrageenan-induced rat's paw oedema, Pharmacol. Res. 45 (2002) 1–4, https://doi.org/10.1006/PHRS.2001.0856.
[38] R. Chudnovskiy, A. Thompson, K. Tharp, M. Hellerstein, J.L. Napoli, A. Stahl, M. Makishima, Consumption of clarified grapefruit juice ameliorates high-fat diet induced insulin resistance and weight gain in mice, PLoS One 9 (10) (2014) e108408.
[39] I. Erlund, E. Meririnne, G. Alfthan, A. Aro, Plasma kinetics and urinary excretion of the flavanones naringenin and hesperetin in humans after ingestion of orange juice and grapefruit juice, J. Nutr. 131 (2001) 235–241, https://doi.org/10.1093/JN/131.2.235.
[40] L. Guo, K. Fukuda, T. Ohta, Y.Y. Disposition, Role of furanocoumarin derivatives on grapefruit juice-mediated inhibition of human CYP3A activity, Drug Metab. Dispos. 28 (2000) 766–771.
[41] J. Kiani, S.Z. Imam, Medicinal importance of grapefruit juice and its interaction with various drugs, Nutr. J. 6 (2007) 1–9, https://doi.org/10.1186/1475-2891-6-33.
[42] K. Seden, L. Dickinson, S. Khoo, D. Back, Grapefruit-drug interactions, Drugs. 70 (2010) 2373–2407, https://doi.org/10.2165/11585250-000000000-00000.
[43] M.T. San Miguel, J.A. Martínez, E. Vargas, Food-drug interactions in the summary of product characteristics of proprietary medicinal products, Eur. J. Clin. Pharmacol. 61 (2005) 77–83, https://doi.org/10.1007/S00228-004-0846-9.
[44] M. Jehangir, D. Ahmed, M. Ahmed, M. Naeem, Validated stability indicating HPLC and UFLC assay for the determination of azithromycin: application to solid dosage and biological samples, Lat. Am. J. Pharm. 39 (2020) 1491–1499.
[45] D.R. Sahoo, S. Sahoo, Development and validation of a rapid solid-phase extraction: ultrafast liquid chromatographic method for the estimation of azithromycin and its major related substances in human plasma and dosage forms using a novel polyfunctional silyl reagent-bonded Co, Chromatographia 82 (2019) 1489–1500, https://doi.org/10.1007/s10337-019-03768-z.
[46] V. Sok, F. Marzan, D. Gingrich, F. Aweeka, L. Huang, P. Avino, Development and validation of an LC-MS/MS method for determination of hydroxychloroquine, its two metabolites, and azithromycin in EDTA-treated human plasma, PLoS One 16 (3) (2021) e0247356.
[47] M. Filist, K. Buś-Kwaśnik, H. Ksycińska, P.J. Rudzki, Simplified LC-MS/MS method enabling the determination of azithromycin in human plasma after a low 100mg dose administration, J. Pharm. Biomed. Anal. 100 (2014) 184–189, https://doi.org/10.1016/j.jpba.2014.07.015.
[48] L. Hu, T. Zhou, J. Feng, H. Jin, Y. Tao, D. Luo, S. Mei, Y.I. Lee, A rapid and sensitive molecularly imprinted electrochemiluminescence sensor for Azithromycin determination in biological samples, J. Electroanal. Chem. 813 (2018) 1–8, https://doi.org/10.1016/j.jelechem.2018.02.010.
[49] I.A. Stoian, B.C. Iacob, C.L. Dudaș, L. Barbu-Tudoran, D. Bogdan, I.O. Marian, E. Bodoki, R. Oprean, Biomimetic electrochemical sensor for the highly selective detection of azithromycin in biological samples, Biosens. Bioelectron. 155 (2020), 112098, https://doi.org/10.1016/j.bios.2020.112098.
[50] S.M. El-Adl, M.E. El-sadek, M.H. Hassan, Spectrophotometric analysis of azithromycin and clarithromycin in tablets and human plasma using p-Chloranilic acid, Anal. Chem. Lett. 9 (2019) 362–372, https://doi.org/10.1080/22297928.2018.1483266.
[51] Y. Zhao, L. Couchman, K. Kipper, R. Arya, J.P. Patel, A UHPLC-MS/MS method to simultaneously quantify apixaban, edoxaban and rivaroxaban in human plasma and breast milk: for emerging lactation studies, J. Chromatogr. B Anal. Technol. Biomed. Life Sci. 1144 (2020) 122095.
[52] J. Dzudovic, M.C. Sakac, M. Antunovic, A. Repic, S. Obradovic, S. Djordjevic, J. Savic, B. Dzudovic, Development and validation of LC-MS/MS method for determination of plasma apixaban, Acta Chromatogr. 34 (3) (2022) 332–337.
[53] A. Chernonosov, L. Aksenova, V. Koval, The development of a liquid chromatography high-resolution mass spectrometric method for apixaban quantification in dried plasma spots in parallel reaction monitoring mode, Processes 9 (2021) 1–12, https://doi.org/10.3390/pr9030450.
[54] K. Shaikh, A. Mungantiwar, S. Halde, N. Pandita, A liquid chromatography-tandem mass spectrometry method for the determination of apixaban in human plasma and its application to pharmacokinetics studies in the Indian population, Anal. Methods 13 (2021) 3693–3704, https://doi.org/10.1039/d1ay00837d.
[55] M.L. Ahmed Baig, S.A. Ali, A validated LC-MS/MS method for the estimation of apixaban in human plasma, J. Appl. Pharm. Sci. 7 (2017) 44–52, https://doi.org/10.7324/JAPS.2017.70406.
[56] W.-l. Zhang, D. Lou, D.-T. Zhang, Y. Zhang, H.-J. Huang, Determination of rivaroxaban, apixaban and edoxaban in rat plasma by UPLC–MS/MS method, J. Thromb. Thrombolysis 42 (2) (2016) 205–211.
[57] F. Gouveia, J. Bicker, J. Santos, M. Rocha, G. Alves, A. Falcão, A. Fortuna, Development, validation and application of a new HPLC-DAD method for simultaneous quantification of apixaban, dabigatran, edoxaban and rivaroxaban in human plasma, J. Pharm. Biomed. Anal. 181 (2020), 113109, https://doi.org/10.1016/j.jpba.2020.113109.
[58] F. Bianchi, M. Mattarozzi, N. Riboni, P. Mora, S.A. Gandolfi, M. Careri, A rapid microextraction by packed sorbent – liquid chromatography tandem mass spectrometry method for the determination of dexamethasone disodium phosphate and dexamethasone in aqueous humor of patients with uveitis, J. Pharm. Biomed. Anal. 142 (2017) 343–347, https://doi.org/10.1016/j.jpba.2017.05.025.
[59] M.S. Ferreira, C.R. Marquez, D.A. Dos Santos, J.J. Gabbai, A.C. Martho, A. H. Yamanouchi Brandão, K.A. Barella, M.F. Riccio, A.C. Noboli, P.S. Júnior, Validation of direct method to quantify dexamethasone in human aqueous humor by LC-MS/MS, Bioanalysis 10 (2018) 1361–1370, https://doi.org/10.4155/bio-2018-0079.
[60] Y. Yuan, X. Zhou, J. Li, S. Ye, X. Ji, L. Li, T. Zhou, W. Lu, Development and validation of a highly sensitive LC-MS/MS method for the determination of dexamethasone in nude mice plasma and its application to a pharmacokinetic study, Biomed. Chromatogr. 29 (2015) 578–583, https://doi.org/10.1002/bmc.3316.
[61] W. Gong, S. Liu, P. Xu, M. Fan, M. Xue, Simultaneous quantification of diazepam and dexamethasone in plasma by high-performance liquid chromatography with tandem mass spectrometry and its application to a pharmacokinetic comparison between normoxic and hypoxic rats, Molecules 20 (2015) 6901–6912, https://doi.org/10.3390/molecules20046901.
[62] J. Gu, J. Wang, A. Krishna, L. Xu, S. Stewart, Y. Wang, P.J. Faustino, D. Shakleya, Simultaneous quantification of dexamethasone and 6β-hydroxydexamethasone in rabbit plasma, aqueous and vitreous humor, and retina by UHPLC-MS/MS, Bioanalysis 13 (2021) 1051–1062, https://doi.org/10.4155/bio-2021-0088.
[63] J.M. Hawley, L.J. Owen, M. Debono, J. Newell-Price, B.G. Keevil, Development of a rapid liquid chromatography tandem mass spectrometry method for the quantitation of serum dexamethasone and its clinical verification, Ann. Clin. Biochem. 55 (2018) 665–672, https://doi.org/10.1177/0004563218766566.
[64] H.M. Maher, N.Z. Alzoman, M.M. Alshehri, H.I. Aljohar, S. Shehata, M. Alossaimi, N.O. Abanmy, Simultaneous determination of dexamethasone and lenalidomide in rat plasma by solid phase extraction and ultra-performance liquid chromatography-tandem mass spectrometry: application to pharmacokinetic studies, RSC Adv. 5 (2015) 98600–98609, https://doi.org/10.1039/c5ra22339c.
[65] S. Alimohammadi, M.A. Kiani, M. Imani, H. Rafii-Tabar, P. Sasanpour, Electrochemical determination of dexamethasone by graphene modified electrode: experimental and theoretical investigations, Sci. Rep. 9 (2019) 1–10, https://doi.org/10.1038/s41598-019-47420-0.
[66] A.M. Akhoundi-Khalafi, M.R. Shishehbore, A new technique for quantitative determination of dexamethasone in pharmaceutical and biological samples using kinetic spectrophotometric method, Int. J. Anal. Chem. 2015 (2015) 1–6.
[67] P.V. Duse, K.G. Baheti, Bioanalytical method development and validation for the determination of Favipiravir in spiked human plasma by using RP-HPLC, J. Pharm. Res. Int. 33 (2021) 275–281, https://doi.org/10.9734/jpri/2021/v33i47a33014.
[68] M. Hailat, I. Al-Ani, M. Hamad, Z. Zakareia, W, Abu Dayyih, Development and validation of a method for quantification of Favipiravir as covid-19 management in spiked human plasma, Molecules. 26 (2021) 1–11, https://doi.org/10.3390/molecules26133789.
[69] I.A. Abdallah, S.F. Hammad, A. Bedair, A.H. Elshafeey, F.R. Mansour, Determination of favipiravir in human plasma using homogeneous liquid–liquid microextraction followed by HPLC/UV, Bioanalysis 14 (4) (2022) 205–216.

[70] I.A. Abdallah, S.F. Hammad, A. Bedair, F.R. Mansour, Menthol-assisted homogenous liquid-liquid microextraction for HPLC/UV determination of favipiravir as an antiviral for COVID-19 in human plasma, J. Chromatogr. B Anal. Technol. Biomed. Life Sci. 1189 (2022) 123087.
[71] S. Megahed, A. Habîb, S. Hammad, A. Kamal, Chemometric approach based on factorial and box-Behnken designs for determination of Anti coronavirus drug; Favipiravir in bulk and spiked human plasma by green HPLC method, Turkish, J. Anal. Chem. 3 (2021) 70–78, https://doi.org/10.51435/turkjac.963652.
[72] D. Eryavuz Onmaz, S. Abusoglu, M. Onmaz, F.H. Yerlikaya, A. Unlu, Development and validation of a sensitive, fast and simple LC-MS / MS method for the quantitation of Favipiravir in human serum, J. Chromatogr. B Anal. Technol. Biomed. Life Sci. 1176 (2021) 122768.
[73] M.I. Morsy, E.G. Nouman, Y.M. Abdallah, M.A. Zainelabdeen, M.M. Darwish, A. Y. Hassan, A.S. Gouda, M.R. Rezk, A.M. Abdel-Megied, H.M. Marzouk, A novel LC-MS/MS method for determination of the potential antiviral candidate Favipiravir for the emergency treatment of SARS-CoV-2 virus in human plasma: application to a bioequivalence study in Egyptian human volunteers, J. Pharm. Biomed. Anal. 199 (2021), 114057, https://doi.org/10.1016/j.jpba.2021.114057.
[74] M.R. Rezk, K.A. Badr, N.S. Abdel-Naby, M.M. Ayyad, A novel, rapid and simple UPLC–MS/MS method for quantification of Favipiravir in human plasma: application to a bioequivalence study, Biomed. Chromatogr. 35 (2021) 1–9, https://doi.org/10.1002/bmc.5098.
[75] S.M. Megahed, A.A. Habib, S.F. Hammad, A.H. Kamal, Experimental design approach for development of spectrofluorimetric method for determination of favipiravir; a potential therapeutic agent against COVID-19 virus: application to spiked human plasma, Spectrochim. Acta - Part A Mol. Biomol. Spectrosc. 249 (2021) 119241.
[76] D.A.M. Noureldeen, J.M. Boushra, A.S. Lashien, A.F.A. Hakiem, T.Z. Attia, Novel environment friendly TLC-densitometric method for the determination of anti-coronavirus drugs "Remdesivir and Favipiravir": green assessment with application to pharmaceutical formulations and human plasma, Microchem. J. 174 (2022), 107101, https://doi.org/10.1016/j.microc.2021.107101.
[77] M.A. Mohamed, G.M.G. Eldin, S.M. Ismail, N. Zine, A. Elaissari, N. Jaffrezic-Renault, A. Errachid, Innovative electrochemical sensor for the precise determination of the new antiviral COVID-19 treatment Favipiravir in the presence of coadministered drugs, J. Electroanal. Chem. 895 (2021), 115422, https://doi.org/10.1016/j.jelechem.2021.115422.
[78] M. Mehmandoust, Y. Khoshnavaz, M. Tuzen, N. Erk, Voltammetric sensor based on bimetallic nanocomposite for determination of Favipiravir as an antiviral drug, Microchim. Acta 188 (2021) 434, https://doi.org/10.1007/s00604-021-05107-2.
[79] K. Habler, M. Brügel, D. Teupser, U. Liebchen, C. Scharf, U. Schönermarck, M. Vogeser, M. Paal, Simultaneous quantification of seven repurposed COVID-19 drugs remdesivir (plus metabolite GS-441524), chloroquine, hydroxychloroquine, lopinavir, ritonavir, favipiravir and azithromycin by a two-dimensional isotope dilution LC–MS/MS method in human serum, J. Pharm. Biomed. Anal. 196 (2021), 113935, https://doi.org/10.1016/j.jpba.2021.113935.
[80] Food and Drug Administration, Guidance for Industry: Bioanalytical Method Validation, Food and Drug Administration, Maryland, USA, 2018.
[81] European Medicines Agency, Guideline on Bioanalytical Method Validation, (2011).
[82] H. Kizilkaya, V. Gençer, The effect of prophylactic vitamin C use on COVID-19 infection, J. Heal. Sci. Med. 5 (2022) 13–17. https://doi.org/10.32322/jhsm.948014.
[83] Grapefruit Juice and Some Drugs Don't Mix | FDA, (2021). https://www.fda.gov/consumers/consumer-updates/grapefruit-juice-and-some-drugs-dont-mix.
[84] K. He, J.M. Luettgen, D. Zhang, B. He, J.E. Grace, B. Xin, D.J.P. Pinto, P.C. Wong, R.M. Knabb, P.Y.S. Lam, R.R. Wexler, S.J. Grossman, Preclinical pharmacokinetics and pharmacodynamics of apixaban, a potent and selective factor Xa inhibitor, Eur. J. Drug Metab. Pharmacokinet. 36 (3) (2011) 129–139.
[85] M.A. El-Kader, Evaluation of azithromycin induced cardiotoxicity in male albino rats and the possible protective role of nigella sativa oil, Egypt, J. Histol. 43 (2020) 465–476. https://doi.org/10.21608/ejh.2019.13772.1138.
[86] K. Hosohata, M. Uesugi, S. Hashi, M. Hosokawa, K. Inui, K. Matsubara, K. Ogawa, Y. Fujimoto, T. Kaido, S. Uemoto, S. Masuda, Drug Metabolism and Pharmacokinetics (DMPK) Advance Publication by J-STAGE, Drug Metab. Pharmacokinet. (DMPK)2. 450 (2012) 1–31.
[87] S.J.F. Kaptein, S. Jacobs, L. Langendries, L. Seldeslachts, S. ter Horst, L. Liesenborghs, B. Hens, V. Vergote, E. Heylen, K. Barthelemy, E. Maas, C. De Keyzer, L. Bervoets, J. Rymenants, T. Van Buyten, X. Zhang, R. Abdelnabi, J. Pang, R. Williams, H.J. Thibaut, K. Dallmeier, R. Boudewijns, J. Wouters, P. Augustijns, N. Verougstraete, C. Cawthorne, J. Breuer, C. Solas, B. Weynand, P. Annaert, I. Spriet, G. Vande Velde, J. Neyts, J. Rocha-Pereira, L. Delang, Favipiravir at high doses has potent antiviral activity in SARS-CoV-2–infected hamsters, whereas hydroxychloroquine lacks activity, Proc. Natl. Acad. Sci. USA 117 (43) (2020) 26955–26965.
[88] C. Stöllberger, J. Finsterer, Relevance of P-glycoprotein in stroke prevention with dabigatran, rivaroxaban, and apixabanRelevanz von P-Glykoprotein in der Schlaganfallprävention mit Dabigatran, Rivaroxaban und Apixaban, Herz 40 (S2) (2015) 140–145.
[89] J.M. Walenga, C. Adiguzel, Drug and dietary interactions of the new and emerging oral anticoagulants, Int. J. Clin. Pract. 64 (2010) 956–967, https://doi.org/10.1111/j.1742-1241.2009.02286.x.
[90] J.M. Pascussi, L. Drocourt, S. Gerbal-Chaloin, J.M. Fabre, P. Maurel, M.J. Vilarem, Dual effect of dexamethasone on CYP3A4 gene expression in human hepatocytes. Sequential role of glucocorticoid receptor and pregnane X receptor, Eur. J. Biochem. 268 (2001) 6346–6358. https://doi.org/10.1046/J.0014-2956.2001.02540.X.
[91] H. Heidbuchel, P. Verhamme, M. Alings, M. Antz, H.C. Diener, W. Hacke, J. Oldgren, P. Sinnaeve, A.J. Camm, P. Kirchhof, Updated European Heart Rhythm Association Practical Guide on the use of non-vitamin K antagonist anticoagulants in patients with non-valvular atrial fibrillation, Europace 17 (2015) 1467–1507, https://doi.org/10.1093/EUROPACE/EUV309.
[92] W. Byon, S. Garonzik, R.A. Boyd, C.E. Frost, Apixaban: a Clinical pharmacokinetic and pharmacodynamic review, Clin. Pharmacokinet. 58 (2019) 1265–1279, https://doi.org/10.1007/s40262-019-00775-z.
[93] J.F. Westphal, Macrolide – induced clinically relevant drug interactions with cytochrome P-450A (CYP) 3A4: an update focused on clarithromycin, azithromycin and dirithromycin, Br. J. Clin. Pharmacol. 50 (2000) 285, https://doi.org/10.1046/J.1365-2125.2000.00261.X.
[94] T. Lan, A. Rao, J. Haywood, C.B. Davis, C. Han, E. Garver, P.A. Dawson, Interaction of macrolide antibiotics with intestinally expressed human and rat organic anion-transporting polypeptides, Drug Metab. Dispos. 37 (2009) 2375–2382, https://doi.org/10.1124/DMD.109.028522.
[95] M. Sugie, E. Asakura, Y.L. Zhao, S. Torita, M. Nadai, K. Baba, K. Kitaichi, K. Takagi, K. Takagi, T. Hasegawa, Possible involvement of the drug transporters P glycoprotein and multidrug resistance-associated protein Mrp2 in disposition of azithromycin, Antimicrob. Agents Chemother. 48 (2004) 809–814, https://doi.org/10.1128/AAC.48.3.809-814.2004.
[96] A. Galetin, H. Burt, L. Gibbons, J.B. Houston, Prediction of time-dependent CYP3A4 drug-drug interactions: impact of enzyme degradation, parallel elimination pathways, and intestinal inhibition, Drug Metab. Dispos. 34 (2006) 166–175, https://doi.org/10.1124/DMD.105.006874.
[97] A. Courtois, L. Payen, A. Guillouzo, O. Fardel, Up-regulation of multidrug resistance-associated protein 2 (MRP2) expression in rat hepatocytes by dexamethasone, FEBS Lett. 459 (1999) 381–385, https://doi.org/10.1016/S0014-5793(99)01295-8.
[98] S. Manceau, X. Declèves, C. Giraud, F. Batteux, C. Chéreau, S. Chouzenoux, J.-M. Scherrmann, B. Weill, J.-Y. Perrot, J.-M. Tréluyer, Expression and induction by dexamethasone of ABC transporters and nuclear receptors in a human T-lymphocyte cell line, Taylor Fr. 24 (2012) 48–55, https://doi.org/10.1179/1120009X12Z.00000000010.
[99] E. Mishima, N. Anzai, M. Miyazaki, T. Abe, Uric acid elevation by Favipiravir, an antiviral drug, Tohoku J. Exp. Med. 251 (2020) 87–90, https://doi.org/10.1620/TJEM.251.87.